LA-UR-21-22576
Approved for public release; distribution is unlimited.

Title: Imaging APO-BMI with Micro X-ray Computed Tomography (CT)

Author(s): Young, Steven Glen

Intended for: Report

Issued: 2021-03-16

Imaging APO-BMI with Micro X-ray Computed Tomography (CT)

Steven G. Young*

Los Alamos National Laboratory, PO Box 1663, MS E549, Los Alamos, NM 87545.

KEYWORDS: APO-BMI, Micro X-ray Computed Tomography, Load Cell.

ABSTRACT: APO-BMI is a high-strength, high-temperature, and low-density foam comprised of 1,2-bis(2-aminophenylthio)ethane (APO-Link, formerly Apocure-601) and 4,4'-bismaleimidodiphenylmethane (BMI) that is used structural applications within the aerospace and weapons manufacturing sectors.[1,2] APO-link is the diamine reagent used to synthesize BMI, a thermosetting resin. This resin can remain in a molten, flowing state for an extended period of time before cross-linking, allowing addition of glass or carbon microballoons to form its final structure. A portion of the current project was to observe the thermal effects on the structural integrity of the foam associated with exposure to an ion beam. Features within the foam were imaged using micro X-ray computed tomography (CT). The resulting imaging provided evidence that microballoon structure remained mostly intact at the points of failure, indicating that the failure of the material was occurring in the binder material.

Scheme 1. Synthesis of APO-BMI from 1,2-bis(2-aminophenylthio)ethane (APO-Link) and maleic anhydride.[3]

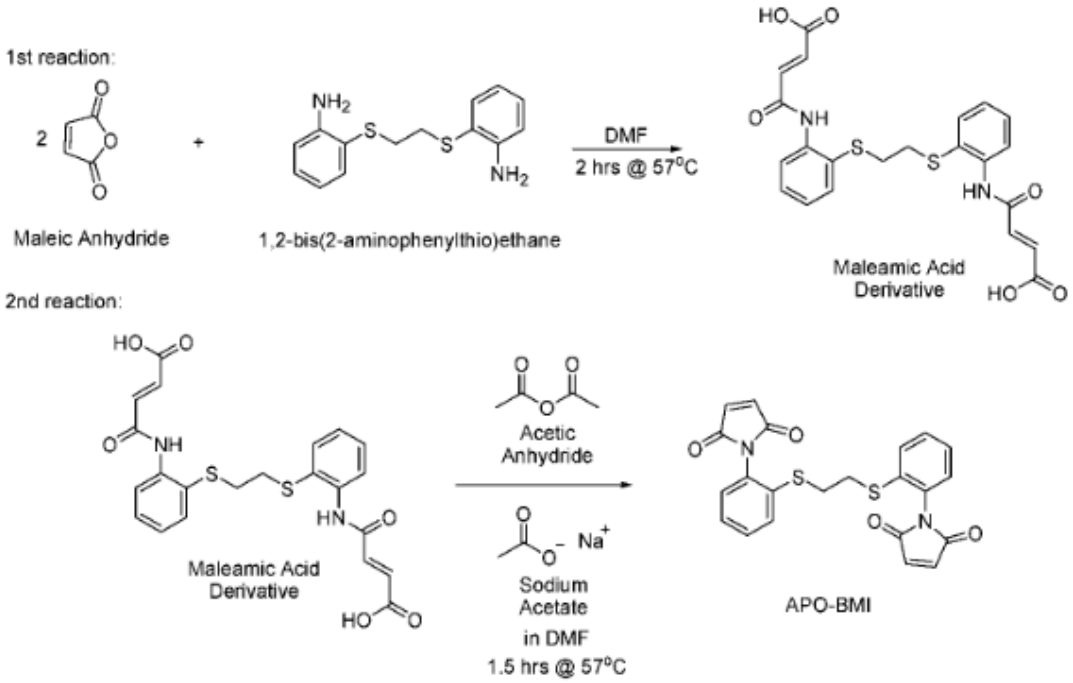

Developed in the late 1970's, APO-Link (formerly APO-Cure-601) has been utilized to synthesize the bismaleimide resin, APO-BMI.[2] This resin can be mixed with glass or carbon microballoons (glass microballoons are observable in Figure 1) prior to cooling, forming a syntactic foam that demonstrates good compressive strength and high temperature tolerance at a low density. APO-BMI has several advantages over previously utilized syntactic foam formulations. The use of APO-Link as a reagent results in fewer adverse toxicological or physiological concerns associated with the synthesis process and the raw materials were more readily available. APO-BMI was more cost effective, eliminating the need for melt-blending and grinding the

resulting blend. Finally, the wide temperature range between melting (120° C) and curing (230° C)[4] gave the material good molding capability.

The ultimate goal of this project is to observe the effects of compressive forces on various carbon microballoon APO-BMI samples in situ, using micro X-ray computed tomography (CT) with a load cell. While awaiting the arrival of sample material, and to build proficiency with the instrumentation, a series of images were collected on a collection of glass microballoon APO-BMI samples that were irradiated with either an electron beam or an ion beam. These samples were evaluated for structural and compositional changes associated with their exposure. Several samples that were surface-coated with metal were also imaged to determine the extent of coverage and thickness of the metal coating.

X-ray CT is a non-destructive imaging process that produces a three-dimensional image of the internal surfaces of an object by reconstructing a series of layered slices through the material being analyzed. These slices are obtained by directing X-rays at an object at multiple orientations while measuring the changes in intensity at the instruments detector.[5] These changes in intensity, referred to as attenuation, occur due to signal scattering or absorption as a function of X-ray energy, path length of travel, and the material's linear attenuation coefficient. Attenuation of X-ray signals occurs mostly through three physical processes; photoelectric effect (PE), Compton scattering (CS), and pair production (PP). In PE absorption, an inner electron absorbs the entire energy of the incoming X-ray photon, causing the electron to be ejected from its orbit. Compton scattering occurs when an outer electron absorbs a portion of the photon's energy, ejecting the electron and redirecting the photon. Pair production occurs when the X-ray photon interacts with the nucleus, creating a positron and electron. PE is predominant at lower source voltage settings and CS is more prevalent at higher voltage settings. As X-rays reach the detector and interact with the detector's scintillating materials, the X-ray photons are converted to visible wavelengths, which are counted by the detector. Higher-z materials attenuate a greater number of X-ray photons, producing brighter signatures in the resulting reconstructed images.

The instrument used for imaging was the Carl Zeiss Xradia 520 Versa with at tungsten filament source capable of operating between 30 and 160 kilovolts potential, up to a maximum power of 10 Watts.[6] This system is fitted with a variety of objectives, 0.4X, 4X, 10X, and 20X, along with a flat-panel detector for a larger field of view. Samples were mounted onto a stage capable of 360° rotation. Typical imaging conditions were: 60 kVp, 5W, 4X mag, 1.66 µm voxel size (unless otherwise noted).

Seven samples were exposed to an electron beam at the Naval Research Laboratories, GAMBLE II facility, which induced rapid heating of the material, causing the material to fracture. These fractured pieces were imaged to determine the extent of structural damage that occurred at the points of failure (Figure 1).

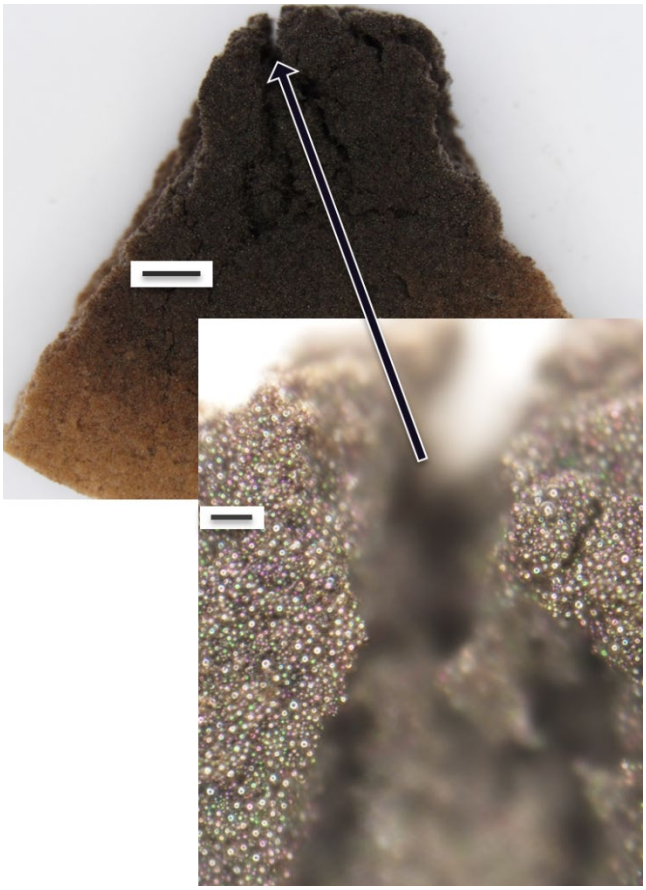

Figure 1. Microphotograph image of fractured piece of APO-BMI sample following exposure to electron beam. Scalebars: 1000 µm (Top) and 100 µm (Inset).

While the extent of damage caused by the electron beam varied between samples, all samples exhibited consistent means of material failure when analyzed with micro X-ray CT. Figure 2 is a reconstructed slice of the sample shown above, it shows that common point of failure in the material occurs predominantly in the binder material, while the glass microballoons remain largely intact. The most heavily-damaged sample (Figure 3) fragmented to the point that only a fraction of the original material was recovered. During CT imaging, a higher occurrence of high-z material was noted in the radiographs. These anomalies were confirmed by the experimenter, stating that the sample assembly was also damaged during that portion of the experiment (Figure 4). In an effort to further visualize the surface at the point of fracture, three-dimensional images were reconstructed from the CT data. Figure 5 shows the digital three-dimensional image that was created, which allowed for the creation of a video panning around the material before slicing through at the fracture surface, shown in Figure 6. This allowed an in-depth observation of each layer along the face of the material failure.

Two additional APO-BMI samples were exposed to ion beam radiation. These samples appeared to have minimal structural damage in the glass microbeads, which was confirmed through CT imaging.

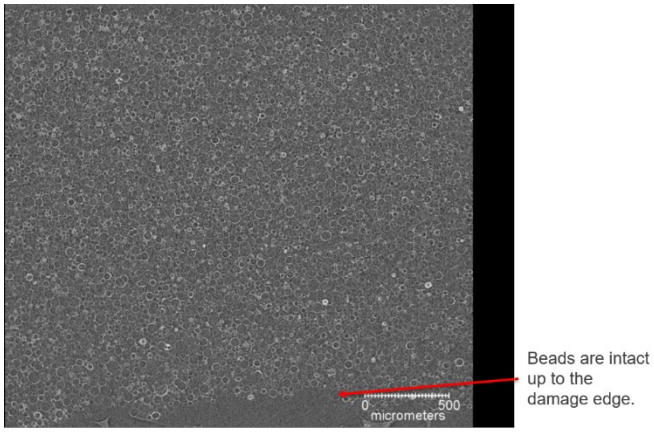

Figure 2. XZ slice indicating that the beads are intact at and below the damaged surface of the APO-BMI.

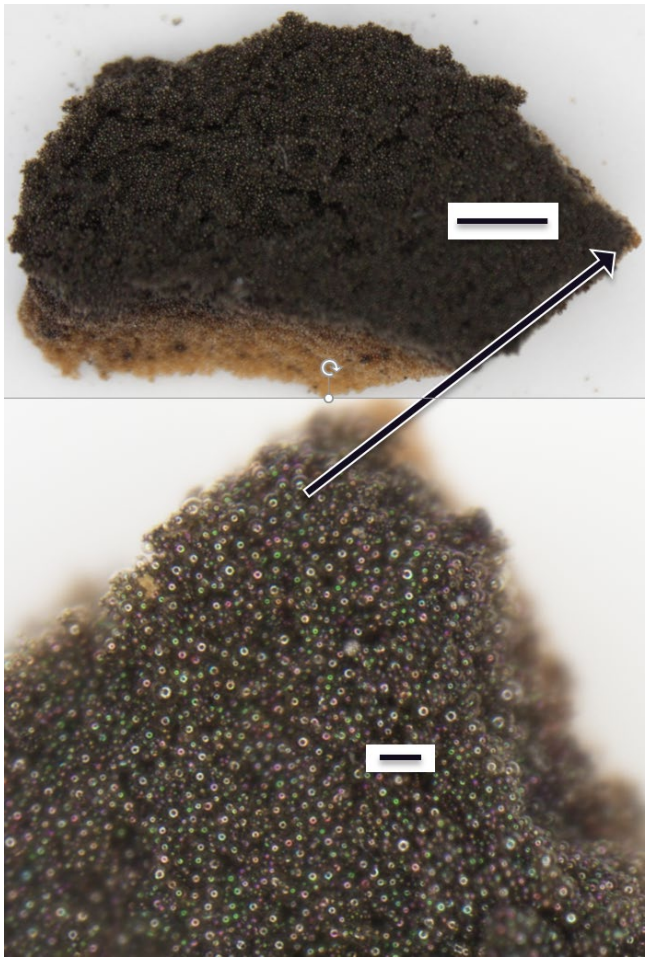

Figure 3. Microphotograph of heavily-damaged APO-BMI fragment. Scalebars: 1000 μm (Top) and 100 μm (Bottom).

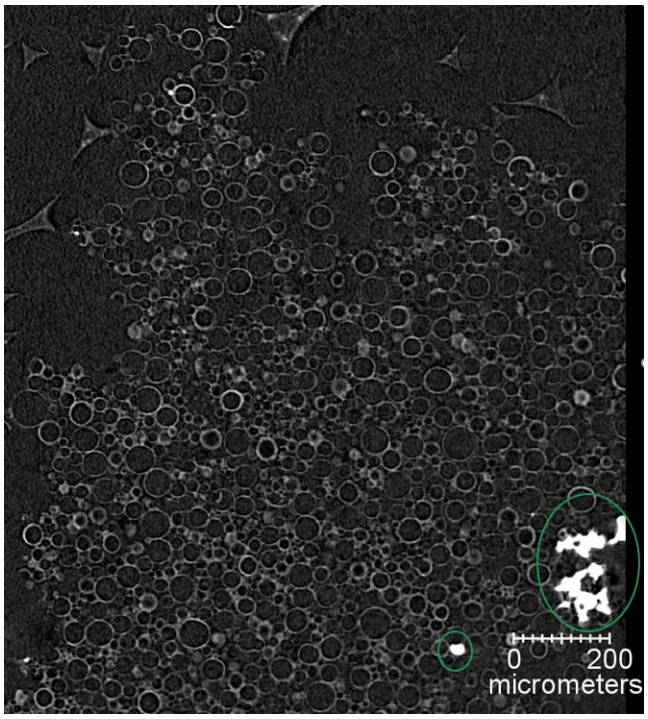

Figure 4. A reconstructed slice of the heavily-damaged APO-BMI sample (from Figure 3) with noted high-z material embedded throughout and intact beads.

Based on the analysis of the damaged APO-BMI samples, it was clear that source of the material failure occurs in the binder material and that the glass microballoons remain mostly intact. There is little evidence that glass microballoons were affected at any point in the structure, even at the faces of the fractures. As the material heated up quickly in the presence of the electron beam, the binder material charred and became more brittle and friable. The portions of the sample that did not indicate charring appeared to remain structurally intact.

Future work will focus on the in situ compression of these materials to better understand how they respond to mechanical loading and compression[7].

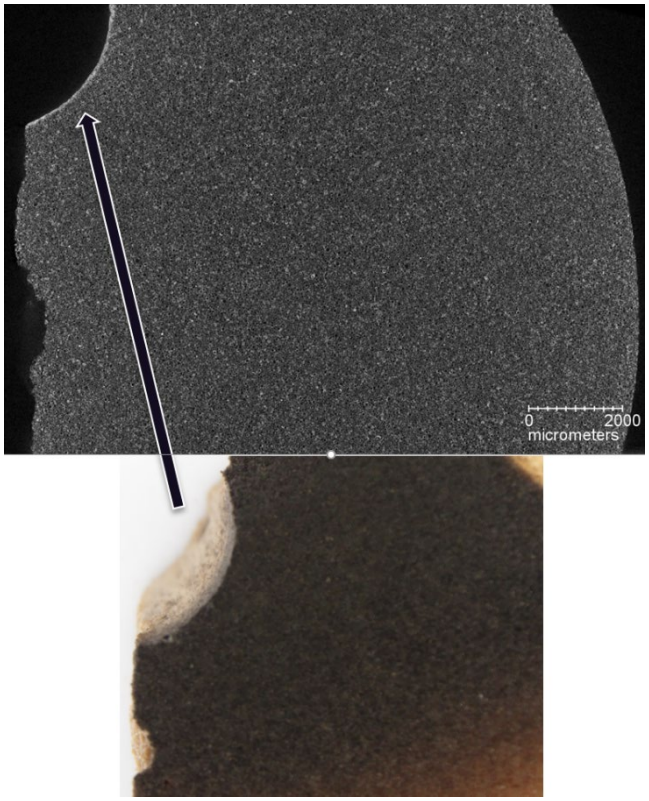

Figure 5. Microphotograph of damaged APO-BMI compared to digitally reconstructed CT image. 7.90 μm voxel size.

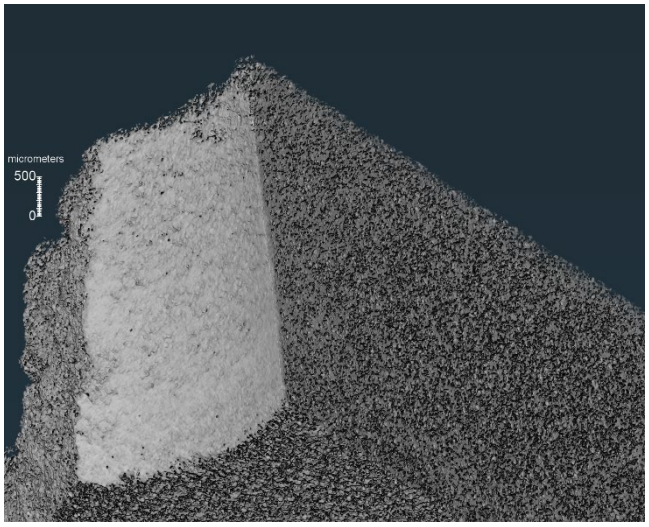

Figure 6. 3D rendering of the contour of the defect allows for observation of structural changes along the face. 7.90 voxel size.

ASSOCIATED CONTENT

N/A

AUTHOR INFORMATION

Corresponding Author

* Steven Young, sgy@lanl.gov, (505)396-1522

Present Address

Los Alamos National Laboratory
PO Box 1663 Mail Stop E549
Los Alamos, NM 87545

Author Contributions

The manuscript was written through contributions of all authors. All authors have given approval to the final version of the manuscript.

Funding Sources

National Nuclear Security Administration (NNSA)

Notes

N/A

ACKNOWLEDGMENT

Special thanks to Brian M. Patterson for his guidance and patience in helping me learn these new imaging techniques.

ABBREVIATIONS

CT, Computed Tomography; PE, photoelectric effect; CS, Compton scattering; PP, pair production.

REFERENCES

1. Daily, C.; Torres, S.; Robison, T.; Bowler, N., Dielectric and kinetic comparison of APO-BMI grades. *High Performance Polymers* **2017,** *30*, 095400831773996.
2. Densmore, C. C., Rebecca *APO-BMI: A Historical Perspective and Recent Efforts Involving Production and Characterization*; Los Alamos National Laboratory: Los Alamos, NM, 2008; pp 1-58.
3. Densmore, C. W., H.; Cohenour, R.; Robison, T.; Hasam, D.; Blossom, J.; Stark, P.; Fuller, E.; Cook, C.; Weber, H., Development of a Scaleable Synthesis for 1,2-Bis(2-aminophenylthio)ethane (APO-Link) Used in the Production of Bismaleimide Resin. *Organic Process Research and Development* **2007,** *11*, 996-1003.
4. Carlisle, K.; Gladysz, G.; Chawla, K.; Koopman, M.; Lewis, M., Characterization of the Binder Phase in a Three-Phase Carbon Microballoon Syntactic Foam. *Cellular Polymers* **2007,** *26*, 157-165.
5. Kyle, J.; Ketcham, R., Application of high resolution X-ray computed tomography to mineral deposit origin, evaluation, and processing. *Ore Geology Reviews* **2015,** *65*, 821-839.
6. Zeiss Your Flexible Imaging Solution. https://www.zeiss.com/content/dam/Microscopy/

us/download/pdf/Products/xradia520versa/xradia-520-versa-product-information.pdf (accessed 2/26).

7. Patterson, B. M.; Cordes, N. L.; Henderson, K.; Xiao, X.; Chawla, N., Data Challenges of In Situ X-Ray Tomography for Materials Discovery. *Materials Discovery and Design: By Means of Data Science and Optimal Learning* **2018,** *280*, 129.

Insert Table of Contents artwork here